

Principal Component Analysis of Distal Femur Based on Statistical Shape Model

Pengyu Zhan¹, Jungang Han¹, Zhe Li², Pei Yang², Jiayu Yang¹ and Dan Han¹

¹Xi'an University of Posts and Telecommunications School of Computing

²The Second Affiliated Hospital of Medical College, Xi'an Jiaotong University Department of Bone and Joint Surgery

Abstract. Knee replacement surgery is currently the primary treatment for end-stage knee osteoarthritis. However, joint replacement surgery still has a high rate of dissatisfaction. One of the reasons is that the prosthesis system does not fit the anatomy of Chinese people. For handling this problem, we study the morphological characteristics of the distal femur, which helps design individualized prosthesis systems. Firstly, the point cloud models of femur samples of Chinese people were derived from the CT scan data by Mimics software. And then, the point cloud models were roughly matched by FPFH (Fast Point cloud Feature Histogram) before the fine registration by ICP (Iterative Closest Point), and by doing so, the average model and correspondence of points were obtained. Finally, the Principal Component Analysis (PCA) was conducted to analyze the morphological characteristics of the distal femur and build the Statistical Shape Model (SSM) of the set of distal femur samples. It is found that the most significant morphological characteristics of the distal femur can be listed in the following order: The volume size, the mediolateral and anteroposterior sizes of the femur, curvature from the femoral shaft to medial and lateral condyle, curvature of the anterior and posterior condyle, width and depth of the trochlear groove, etc. These results will guide the local improvement of the existing prosthesis and provide the basic reference to the new design of the multi-class prosthesis system.

Keywords: femur, fast point feature histogram, iterative closest point, principal component analysis, statistical shape model

1. Introduction

In the past few decades, total knee arthroplasty has developed rapidly and has become the main-stream treatment for end-stage knee osteoarthritis. However, it is reported in the literature that up to 30% of patients are dissatisfied with the joint replacement [1]. The mismatch between the prosthesis and the knee joint anatomy is an important reason for this consequence. Matz et al. showed that the anterior femoral offset, anteroposterior size of the femur, and anterior patellar offset were changed in 40%, 60%, and 71% of patients after TKA, respectively, compared with those before TKA [2]. At the same time, more scholars have also reported the mismatch between the knee joint prosthesis and the knee joint [3]-[5]. Although many prosthetic models are introduced, these models only match the size of the tibiofemoral joint bone shape, and the adaptation of the knee joint with a high degree of shape variation needs to be improved. Therefore, with the development of precision medicine, mining the knowledge of individual shape differences of the knee joint and establishing a more comprehensive prosthesis system accordingly is one of the important directions of osteological surgery.

In recent years, many studies have analyzed the morphology and structure of the distal femur. Iranpou et al. studied the lowest point of the pulley groove and found that the pulley groove has a "double line" shape and a turning point [6]. Thereafter, Chen et al. divided the trochlear groove into 4 categories according to the different turning points, but this study only described the lowest point of the trochlear groove and did not do further research on the overall shape of the trochlear groove, internal and external condyles and knee joint [7]. In another research, Everhart et al. described the shape of the distal femur based on experience and obtained five differences, but did not perform a strict data analysis of the overall shape [8]. Therefore, based on rough registration and precise registration of samples, our study uses the method of active shape modeling to systematically analyze the typical shape and variables of the distal femur.

The statistical shape model (SSM) is a statistical method used to describe the morphological changes of deformable objects. It has been widely used in various fields, including face recognition, model evaluation, etc. [9]-[11]. In the field of medical image analysis, SSM is applied to the segmentation of various structures of the human body, such as the spine, joints, brain, heart, liver, etc. [12]. This method has also been applied to areas of femoral trochlear dysplasia, foot shape, and knee joints of patients with bone joints [13-15]. In addition, SSM is also used for intraoperative navigation. In this paper, SSM is used to analyze the changes in individualized shapes. The purpose is to use the SSM method to analyze the overall shape of the distal femur, obtain the main characteristics of the distal femur shape, and provide a reference for the design of individualized knee joint prostheses. The work in this paper shows that SSM is also a reliable method to analyze the individual differences in the shape of the distal femur of Chinese people.

The other sections of this article are briefed as follows: Section 2 introduces the data set used and the method of registration and SSM; Section 3 shows the experimental results, and analyzes the meaning of the findings of the experimental results; Section 4 summarize the paper.

2. MATERIALS AND METHODS

2.1. Dataset

The data set used by our study comes from clinical CT scan data of 50 subjects in the Second Affiliated Hospital of Xi'an Jiaotong University, China. The image field of CT is 512×512 pixels, the slice thickness and the resolution are 1mm, and 0.625mm×0.625mm respectively. The process of data preprocessing as shown in Figure 1. includes the following steps: Importing the CT data into Mimics using the region growing and reconstruction grid in Mimics for processing [16], and export it in the STL format of three-dimensional data. After using CloudCompare to convert the STL data into a point cloud model, horizontally intercept 65mm at the upper end of the lowest point of the distal femur to construct a model of the distal femur.

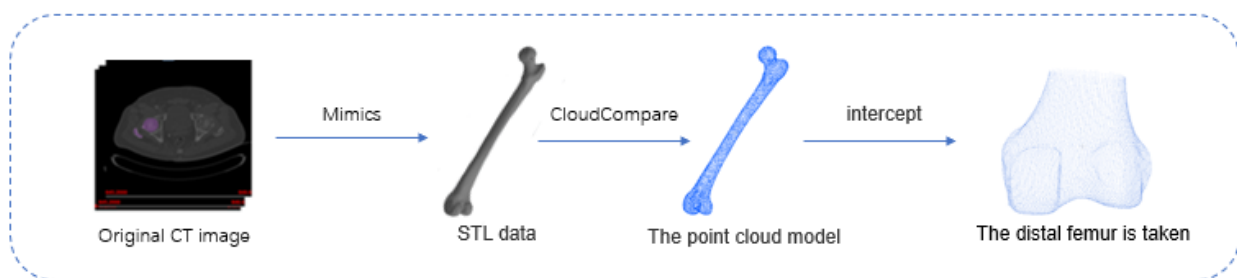


Fig. 1: Data preprocessing steps.

2.2. Method

The statistical shape analysis (SSM) of medical anatomy usually requires the doctors to label the landmarks of samples manually. These are tedious work. Three-dimensional modeling requires even more landmarks than two-dimensional. For doing the work automatically, this study starts from the point cloud data of the samples and determines the correspondence between samples through registration and obtain the landmarks.

Traditional registration methods use ICP (Iterative Closest Point) algorithm [17], [18]. This method achieves registration by minimizing the distance between the two models. However, for different sample data, ICP registration may produce a local optimum. Therefore, we first use FPFH (Fast Point cloud Feature Histogram) to perform coarse registration, providing a better initial state for subsequent fine registration. The point-to-point relationship between the average model and the distal femur sample is obtained through the closest point search, and thus a point distribution model (PDM) is generated. The samples are scaled up or down to reduce the registration error and improve the accuracy of the point-to-relationship.

Point cloud Feature Histogram (PFH) is a robust multi-dimensional feature description. It uses parameters to indicate the spatial difference between a point and its nearest neighbors. The nearest neighbors of points are locally described geometrically in a 3D point cloud dataset [19]. PFH is based on the geometric relationship between points and their neighbors and their estimated normal to describe the point cloud

collection features. For a point cloud P with n points, the complexity of its point feature histogram is $O(n \times k^2)$, where k represents the number of neighbors of the point p in the point cloud P . Radu et al. proposed an optimization algorithm for the point feature histogram, which reduces the computational complexity to $O(n \times k)$ and retains most of the discriminative ability of PFH, which is called fast point feature histogram (FPFH) [20]. Its calculation process is described in the following two steps.

In the first step, only three feature elements between each query point P_q and its neighborhood points are calculated according to formula (1). PFH is to calculate all combinations of feature elements of neighborhood points, while in this step, only feature elements between query points and neighboring points are calculated. Use the “Body text” style for all paragraphs. The following is an example of the “Bullet” style, which you may want to use for lists.

$$\begin{aligned} \alpha &= v \cdot n_j \\ \phi &= \left(u \cdot (p_j - p_i) \right) / \|p_j - p_i\| \\ \theta &= \arctan (w \cdot n_j, u \cdot n_j) \end{aligned} \quad (1)$$

$\langle p_j, p_i \rangle$ ($j \neq i$) is any pair of points in the k neighborhood of p and the estimated normals of p_j and p_i are n_j and n_i respectively (p_i being the point with a smaller angle between its associated normal and the line connecting the points)[20]

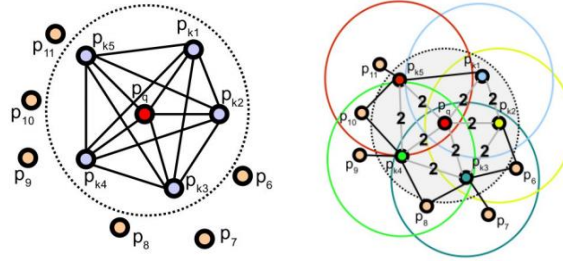


Fig. 2: (a) The influence area of the point feature histogram (b) The influence area of the fast point feature histogram.

As shown in Figure 2, Figure 2(a) is the PFH calculation feature process, that is, the feature value of all combinations of neighboring points (all connections in the figure, including but not limited to the connection between P_q and P_k), Figure 2 (b) is the FPFH calculation feature process, only the feature elements between P_q (query point) and the adjacent point (red line in the right picture) are calculated. It can be seen that the complexity is reduced and we call it Simple Point Feature Histograms (SPFH).

The second step is to re-determine its k neighbors and use the neighboring SPFH values to weight p to get the final FPFH.

$$FPFH(p) = SPF(P) + \frac{1}{k} \sum_{i=1}^k \frac{1}{\omega_k} \cdot SPF(p_k) \quad (2)$$

The establishment of a statistical shape model (SSM) requires the construction of a basic point cloud model set (S_i), also known as a point distribution model (PDM) [21]. Choose any point cloud model of the distal femur as the target model, perform denoising, mesh smoothing and uniform down-sampling operations on the original data, and create a standard node (x_i, y_i, z_i) with 4000 uniform distributions [22]. Perform FPFH rough registration of the remaining samples with the target and automatically align them by a combination of ICP (Iterative closest point) and GPA (Generalized Procrustes analysis) [16]. The point-to-point relationship is established through the nearest point search, and the corresponding point set of the distal femur is constructed, and the average model of the joint is obtained. Construct the covariance matrix (Cov) of each point distribution model through the sample set (S_i) [23].

$$\begin{cases} Cov = \frac{1}{p-1} \sum_{i=1}^p (S_i - \bar{S})(S_i - \bar{S})^T \\ with S_i = (x_1, y_1, z_1, \dots, x_n, y_n, z_n)^T \end{cases} \quad (3)$$

$$\bar{S} = \frac{1}{p} \sum_{i=1}^p S_i, i = 1:p$$

P is the number of sample sets, and n is the number of points for each sample.

In order to make the model more representative, as shown in Figure 3, the first average model is used as the new target model [24], and the second average model is created, which shows more specificity. The typical features of the distal femur are also preserved as much as possible.

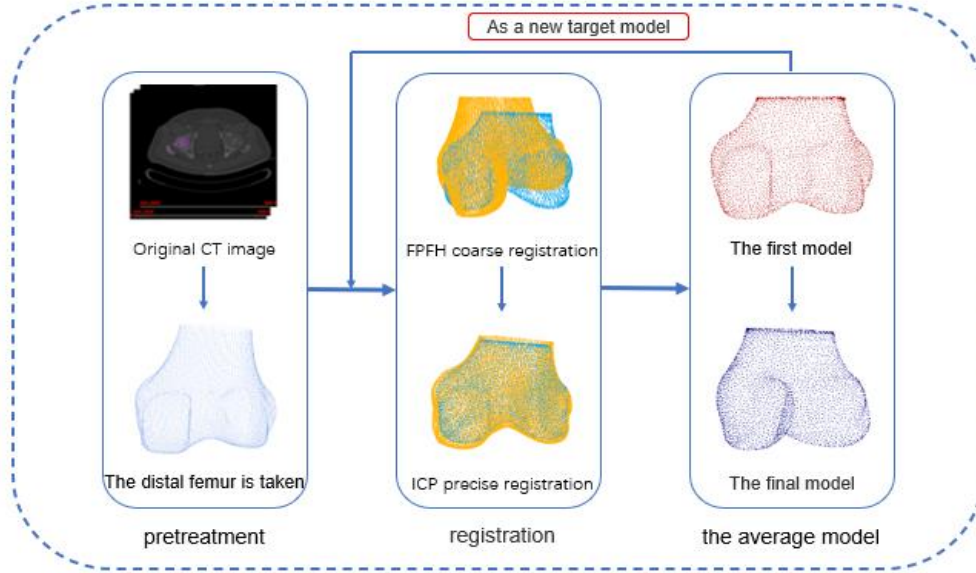


Fig. 3: Process diagram of calculating average model

Principal Component Analysis (PCA) [25] was invented by Carl Pearson in 1901 for analyzing data and establishing mathematical models. The method is essentially to decompose the covariance matrix to obtain the principal components of the data (eigenvectors) and their weights (eigenvalues). Use the principal component analysis method to analyze (3) the covariance matrix of the point distribution model. We use the eigenvalues and eigenvectors of the covariance matrix to obtain the overall geometric characteristics of the distal femur.

$$\begin{cases} \text{eigenvalue} = (\lambda_1, \lambda_2, \dots, \lambda_s), \lambda_1 \geq \lambda_2 \dots \geq \lambda_s \geq 0, \\ \text{eigenvector} = (P_1, P_2, \dots, P_s), \end{cases} \quad (4)$$

Among them, the size of P_i is $1 \times 3n$. The eigenvector corresponding to the largest eigenvalue is the first principal component, the eigenvector corresponding to the second largest eigenvalue is the second principal component, and so on.

Through the average model, eigenvalues and principal components constitute a statistical shape model, and any specific sample can be represented by the statistical shape model, where a_j represents the weight of each principal component [26].

$$\begin{cases} S' = \bar{S} + \sum_{j=1}^s f(\lambda_j) P_j, \\ f(\lambda_j) = a_j \sqrt{\lambda_j}, \end{cases} \quad (5)$$

3. RESULTS

As shown in Figure 4, the eigenvalues of the distal femur are decreasing exponentially; the first eigenvalue is 19280, the second eigenvalue is 5568, the third eigenvalue is 1917, the tenth eigenvalue drops to about 250, the 40th eigenvalue is close to zero. With the attenuation of the eigenvalue amplitude, the influence of the principal components on the average model gradually decreases. Table 1 shows the proportion of the top ten principal components affecting the morphological characteristics of the distal femur.

Starting from the tenth principal component, the influence is less than 1%. Therefore, this article mainly analyzes and describes the first nine principal components.

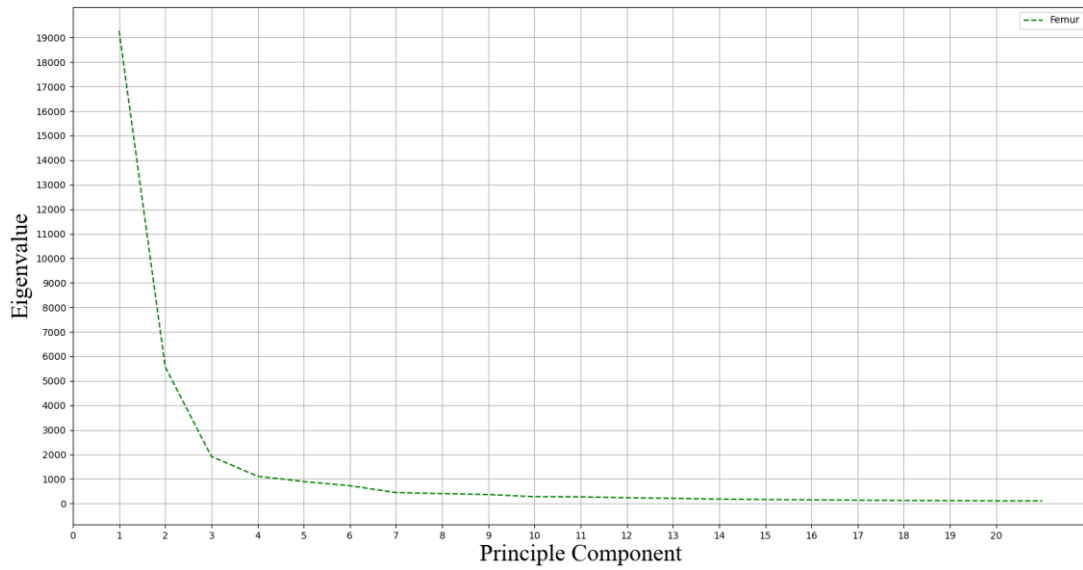


Fig. 4: Femoral PDM covariance matrix eigenvalues between the number of principal components

Table 1: THE INFLUENCE RATIO OF PRINCIPAL COMPONENTS

principal components	PC1	PC2	PC3	PC4	PC5	PC6	PC7	PC8	PC9	PC10
proportion	0.563	0.162	0.056	0.032	0.026	0.021	0.013	0.011	0.010	0.008

As shown in Figure 5, the SSM difference of PC1 is mainly in the size of the entire distal femur, which is similar to the principal components of many statistical shape models. The first principal component usually represents the size. The difference of PC2 is mainly in the size of the mediolateral size of the distal femur and the curvature of the transition from the medial and lateral femoral shaft to the medial and lateral condyles. The difference of PC3 is mainly in the size of the mediolateral and anteroposterior sizes of the distal femur, the curvature of the transition from the medial and lateral femoral shaft to the medial and external condyles, and the curvature of the anterior and posterior condyles. The main difference in PC4 lies in the width and depth of the trochlear groove. The difference in PC5 is mainly in the height of the lateral anterior condyle. The difference of PC6 is mainly the curvature of the transition from the medial and lateral femoral shaft to the medial and lateral condyles and the curvature of the anterior and posterior condyles. The difference in PC7 is mainly the curvature of the transition from the medial and lateral femoral shaft to the medial and lateral condyles. The difference in PC8 is primarily the size and curvature of the medial condyle. The difference in PC9 is mainly in the ratio of the size of the trochlear groove to the mediolateral size of the distal femur.

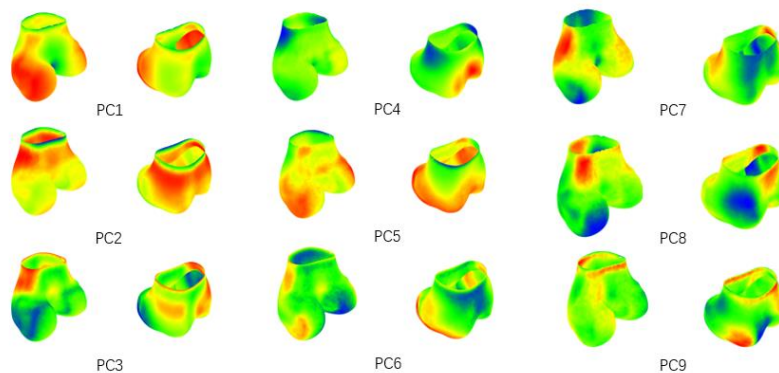


Fig. 5: The three-dimensional surface rendering of the femoral SSM, where the color represents the difference of principal component and the average model.

The prosthesis system provides the basis. Although the current prosthesis system has different models, it is designed based on the different sizes of the same knee joint shape, which leads to the mismatch between the anatomical structure of some people and the prosthesis. This study found many individual differences in the above morphology in the population, mainly focusing on the size and curvature of the femoral condyle and the shape of the trochlear groove. These results will further guide the local improvement of the existing prosthesis and the new multi-classification design of prosthesis.

4. Conclusion

In this study, we used the method of FPFH combined with ICP to construct a statistical shape model. The nine principal components that had the most significant influence on the shape variation of the distal femur were obtained through principal component analysis. We found that the main morphological characteristics of the distal femur were the mediolateral and anteroposterior sizes of the femur, the curvature from the femoral shaft to the medial and lateral condyle, the curvature of the anterior and posterior condyle, the width and depth of the trochlear groove, the ratio of the size of the medial to the lateral condyle, the ratio of the size of the trochlear groove to the distal femur, etc. These results provided an important reference for more individualized prosthesis design.

Previous studies reported the classification of trochlear dysplasia [28]. For the classification of the normal distal femur, more attention had been attributed in recent years. It was reported that the trochlear groove tracking was composed of two parts, which were the laterally orientated proximal and medially orientated distal parts marked by a turning point [6, 7]. And the other literature indicated the difference of the medial and lateral condyles based on clinical experience [8]. Compared with previous studies, this study applied the statistical shape model to analyze the morphological differences of the distal femur from the perspective of the whole distal femur and obtained multiple morphological characteristics with individual differences by principal component analysis. We will further use the principal component characteristics for cluster analysis and perform targeted parameter measurements based on the morphological characteristics suggested by the principal components to provide more reference data for the design of a more comprehensive prosthesis system of the distal femur.

5. References

- [1] F. Canovas, L. Dagneaux, "Quality of life after total knee arthroplasty," *OrthopTraumatol Surg Res*, vol. 104, pp. S41-s6, February 2018.
- [2] J. Matz, J. L. Howard, D. J. Morden, et al., "Do Changes in Patellofemoral Joint Offset Lead to Adverse Outcomes in Total Knee Arthroplasty With Patellar Resurfacing? A Radiographic Review," *J Arthroplasty*, vol. 32, pp. 783-7, March 2017.
- [3] K. M. Varadarajan, H. E. Rubash, G. Li, "Are current total knee arthroplasty implants designed to restore normal trochlear groove anatomy?," *J Arthroplasty*, vol. 26, pp. 274-81, February 2011.
- [4] H. J. Meijerink, M. Barink, C. J. van Loon, et al., "The trochlea is medialized by total knee arthroplasty: an intraoperative assessment in 61 patients," *Acta Orthop*, vol. 78, pp. 123-7, February 2007.
- [5] M. Barink, H. Meijerink, N. Verdonschot, et al., "Asymmetrical total knee arthroplasty does not improve patella tracking: a study without patella resurfacing," *Knee Surg Sports Traumatol Arthrosc*, vol. 15, pp. 184-91, February 2007.
- [6] F. Iranpour, A. M. Merican, W. Dandachli, et al., "The geometry of the trochlear groove," *Clin OrthopRelat Res*, vol. 468, pp. 782-8, March 2010.
- [7] S. Chen, Z. Du, M. Yan, et al., "Morphological classification of the femoral trochlear groove based on a quantitative measurement of computed tomographic models," *Knee Surg Sports TraumatolArthrosc*, vol. 25, pp. 3163-70, October 2017.
- [8] J. S. Everhart, A. M. Chaudhari, D. C. Flanigan, "Creation of a simple distal femur morphology classification system," *J Orthop Res*, vol. 34, pp. 924-31, June 2016.
- [9] N. Sarkalkan, H. Weinans, A. A. Zadpoor, "Statistical shape and appearance models of bones," *Bone*, vol. 60, pp.

129-40, March 2014.

- [10] Y. Yang, H. Zhou, Y. Song, et al., "Identify dominant dimensions of 3D hand shapes using statistical shape model and deep neural network," *Appl Ergon*, vol. 96, pp. 103462, October 2021.
- [11] L. A. Cament, F. J. Galdames, K. W. Bowyer, et al., "Face recognition under pose variation with local Gabor features enhanced by Active Shape and Statistical Models," *Pattern Recognition*, vol. 48, pp. 3371-84, November 2015.
- [12] T. Heimann, H. P. Meinzer, "Statistical shape models for 3D medical image segmentation: a review," *Med Image Anal*, vol. 13, pp. 543-63, August 2009.
- [13] P. Cerveri, A. Belfatto, G. Baroni, et al., "Stacked sparse autoencoder networks and statistical shape models for automatic staging of distal femur trochlear dysplasia," *Int J Med Robot*, vol. 14, pp. e1947, December 2018.
- [14] Z. G. Q. Mei, Justin. Fernandez, Y. Gu, "Three-Dimensional foot shape modelling based on statistical shape model," *Journal of Medical Biomechanics*, vol. 36, pp. 96-101, February 2021.
- [15] T. L. Bredbenner, T. D. Eliason, R. S. Potter, et al., "Statistical shape modeling describes variation in tibia and femur surface geometry between Control and Incidence groups from the osteoarthritis initiative database," *J Biomech*, vol. 43, pp. 1780-6, June 2010.
- [16] F. Chen, Z. Zhao, J. Liu, et al., "Automatic estimation of morphological characteristics of proximal tibia for precise plate treatment using model matching," *Comput Med Imaging Graph*, vol. 81, pp. 101714, April 2020.
- [17] K. S. Shih, C. P. Hsu, C. W. Liu, et al., "Comparison between different screening strategies to determine the statistical shape model of the pelvises for implant design," *Comput Methods Programs Biomed*, vol. 178, pp. 265-73, September 2019.
- [18] T. C. Keating, N. Leong, E. C. Beck, et al., "Evaluation of Statistical Shape Modeling in Quantifying Femoral Morphologic Differences Between Symptomatic and Nonsymptomatic Hips in Patients with Unilateral Femoroacetabular Impingement Syndrome," *Arthrosc Sports Med Rehabil*, vol. 2, pp. e91-e5, April 2020.
- [19] R. B. Rusu, N. Blodow, Z. C. Marton, et al., "Aligning point cloud views using persistent feature histograms," 2008 IEEE/RSJ International Conference on Intelligent Robots and Systems, pp. 3384-3391, September 2008.
- [20] R. B. Rusu, N. Blodow, M. Beetz, "Fast Point Feature Histograms (FPFH) for 3D registration," 2009 IEEE International Conference on Robotics and Automation, pp. 3212-3217, May 2009.
- [21] G. Zheng, M. A. Ballester, M. Styner, et al., "Reconstruction of patient-specific 3D bone surface from 2D calibrated fluoroscopic images and point distribution model," *Med Image ComputComput Assist Interv*, vol. 9, pp. 25-32, 2006.
- [22] Z. Zhu, G. Li, "Construction of 3D human distal femoral surface models using a 3D statistical deformable model," *J Biomech*, vol. 44, pp. 2362-8, September 2011.
- [23] C. Nagel, S. Schuler, O. Dössel, et al., "A bi-atrial statistical shape model for large-scale in silico studies of human atria: Model development and application to ECG simulations," *Med Image Anal*, vol. 74, pp. 102210, August 2021.
- [24] J. T. Lynch, M. T. Y. Schneider, D. M. Perriman, et al., "Statistical shape modelling reveals large and distinct subchondral bony differences in osteoarthritic knees," *J Biomech*, vol. 93, pp. 177-84, August 2019.
- [25] I. T. Jolliffe, J. Cadima, "Principal component analysis: a review and recent developments," *Philos Trans A Math Phys Eng Sci*, vol. 374, pp. 20150202, April 2016.
- [26] T. Y. Tsai, J. S. Li, S. Wang, et al., "Principal component analysis in construction of 3D human knee joint models using a statistical shape model method," *Comput Methods Biomech Biomed Engin*, vol. 18, pp. 721-9, 2015.
- [27] T. F. Cootes, C. J. Taylor, D. H. Cooper, et al., "Active Shape Models-Their Training and Application," *Computer Vision and Image Understanding*, vol. 61, pp. 38-59, January 1995.
- [28] H. Dejour, G. Walch, P. Neyret, et al., "[Dysplasia of the femoral trochlea]," *Rev ChirOrthopReparatriceAppar Mot*, vol. 76, pp. 45-54, 1990.